

The propagation of dislocations in Rayleigh–Bénard rolls and bimodal flow

By J. A. WHITEHEAD

Woods Hole Oceanographic Institution, Woods Hole, Massachusetts 02543

(Received 30 October 1975)

When Rayleigh–Bénard convection is generated under random conditions, the finite amplitude rolls and bimodal flow are observed to possess randomly placed dislocations where the rolls fit together poorly. The dislocations move into the small wavelength convection, and hence provide a size-adjustment mechanism. It is observed that the dimensionless speed of the movement is smaller for larger Prandtl number fluid.

1. Experimental observations

Rayleigh–Bénard convection rolls exist as a stable flow in a closed region of Rayleigh number, wavenumber space as predicted by Busse (1967) and observed by Busse & Whitehead (1971). It has been observed, however, that laboratory convection starting from random initial conditions generally does not fill the full bandwidth predicted by the above theory (Koschmieder 1966, 1969, 1974; Chen & Whitehead 1968; Rossby 1969; Krishnamurti 1970; Willis, Deardorff & Somerville 1972). In addition, three-dimensional numerical calculations predict a wavelength of convection in approximate agreement with laboratory observations (Lipps & Somerville 1971). The departure from uniformly aligned rolls in most experiments and the presence of side walls in all experiments apparently make new size-adjustment mechanisms available and we report here observations of the properties of one such mechanism. The one selected is the ‘junction’ or ‘pinch’ mechanism in which two pairs of cells are locally constricted to one by means of a sudden contraction along their axis. This is described in Busse & Whitehead (*loc. cit.*), and other such contracting structures are described by Willis *et al.* (1972). Figure 1 (plate 1) shows a set of induced rolls where the wavelength makes a sudden contraction from 3 to 2 by means of pinches.

Experimentally, the above flow pattern was generated using the controlled inducing procedure of Chen & Whitehead (1968). In this procedure, a horizontal layer of test fluid in a transparent glass container is held below the critical Rayleigh number while being subjected to bright light from above, which passes through a grid so as to produce a pattern of alternately heated and unheated regions in the test fluid. After a period of time corresponding to at least one thermal time scale d^2/κ , where d is the depth of the fluid and κ is the thermal diffusivity, the temperature difference across the fluid is increased so that the critical Rayleigh number is exceeded. Shortly thereafter the lamp is turned off,

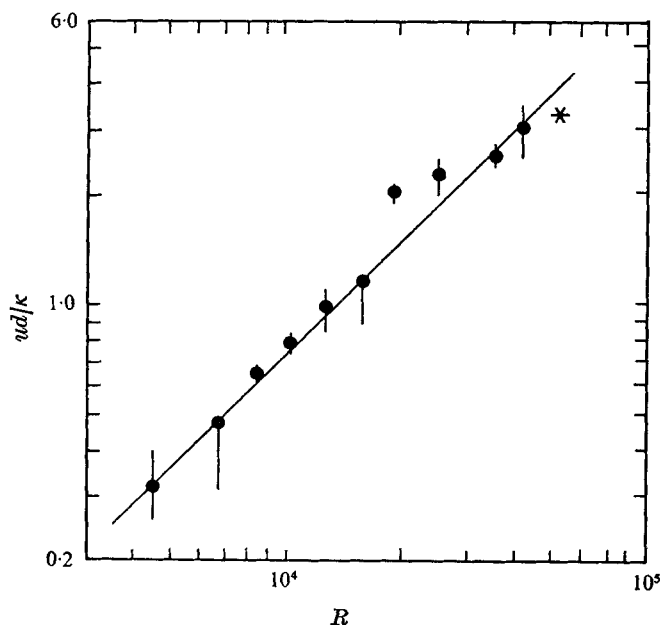


FIGURE 2. Speed of propagation of pinches as a function of Rayleigh number; $Pr = 126$. The point at $R = 20\,000$, which lies furthest off the R^1 line, is the case photographed in figure 1, where one set of rolls has bimodal flow while the other does not. In all other cases the two sets of rolls were both of the same type. The star represents a point where the pinches transformed to a spoke-shaped convection pattern which did not propagate in one direction, but instead nucleated additional spoke-shaped flows which spread in all directions. The vertical bars indicate the extent of the most extreme velocity observations while the solid circles indicate the average velocity from at least 20 samples.

the grid is removed, and observation of the evolving pattern commences using shadowgraph illumination. Generally the pattern observed at that time corresponds to the controlled pattern.

It was possible to use this technique to generate a planar, ordered roll-pinch-roll pattern. The wavenumbers of the two rolls were 3.69 and 2.46, and corresponded to the wavelengths in Busse & Whitehead (1971). In all cases the pinch was observed to move slowly into the small rolls, and hence pinch one pair of rolls out, thus providing a size-adjustment mechanism. The velocity of the pinch was observed to approach a constant value shortly after the final temperature difference across the fluid layer was reached, and was determined by measuring the position of pinches in successive photographs. Figure 1 shows a typical migration. In this case the Rayleigh number was almost exactly 20 000 and the large rolls were in the roll-stable region while the small rolls were in the bimodal stable region. Figure 2 shows the dimensionless velocity of pinches ud/κ as a function of Rayleigh number in silicon oil of Prandtl number 126. The vertical bars indicate the extent of the most extreme velocity observations while the solid circles indicate the average velocity observations from at least 20 samples. A jump in the velocity occurs when the longer wavelength rolls have bimodal flow while the shorter ones do not, as was the case in the photograph, but elsewhere it exhibits a relatively constant logarithmic slope proportional to $R^{1.0}$.

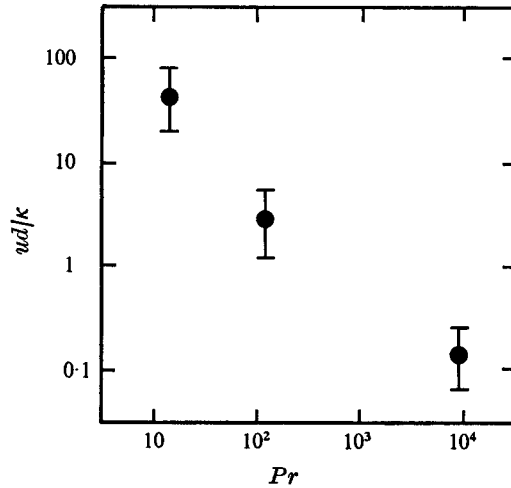


FIGURE 3. Dimensionless speed of propagation of pinches as a function of Prandtl number at a Rayleigh number of $18\,000 \pm 1000$.

A line with slope $R^{1/3}$ is drawn in for visual comparison. At a value of R of above 55 000 the pinch developed into a spoke-shaped structure as described by Busse & Whitehead (1974) and the lateral movement stopped.

A series of experiments was conducted to observe the velocity of pinches for silicon oils with two other Prandtl numbers, 16 and 8600, at Rayleigh numbers of $18\,000 \pm 1000$ and with the same wavenumbers as in the previous case. In the former case, five runs were conducted using both the same apparatus and the same fluid depth as in the experiments at a Prandtl number of 126. The speeds of the central 8 pinches were measured, yielding 40 data points, which were consistent to within $\pm 15\%$. The scatter arose principally because the front of advancing pinches appears to become unstable to one pinch pushing out ahead of its neighbours, and therefore destroying the uniformity of the front. In the latter case, it was necessary to construct a larger apparatus and use a fluid depth of 5 cm because of the large viscosity of the fluid. Three runs were conducted and the velocity of four pinches was measured each time, although the pinches were not as well structured and tended to break down easily in this parameter range. For the three Prandtl numbers, the dimensionless speed of propagation ud/κ is plotted as a function of Prandtl number in figure 3. It is clear that the speed steeply drops off as the Prandtl number is increased.

2. Discussions about dynamics

If length, time and temperature scales of d , d^2/κ and ΔT respectively are used, where d is depth of the fluid, κ is its thermal diffusivity and ΔT is the temperature difference between the bottom and top fluid, the Boussinesq equations become

$$\begin{aligned} \nabla \cdot \mathbf{u} &= 0, \\ Pr^{-1}(\partial \mathbf{u} / \partial t + \mathbf{u} \cdot \nabla \mathbf{u}) &= -\nabla p + \nabla^2 \mathbf{u} + RT \mathbf{k}, \\ \partial T / \partial t + \mathbf{u} \cdot \nabla T &= \nabla^2 T. \end{aligned}$$

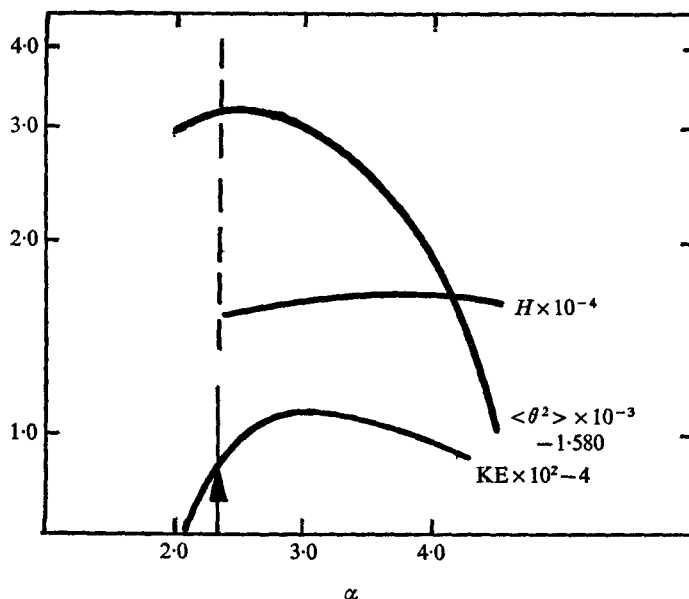


FIGURE 4. Calculated values of the heat flux, kinetic energy and r.m.s. temperature as a function of the wavenumber α . Coefficients were supplied by Busse from the calculation described in Busse (1967). The magnitudes are normalized to fit the data on one graph.

Here, R is the Rayleigh number $g\alpha d^3 \Delta T / \kappa \nu$ and Pr is Prandtl number ν / κ , where g , α and ν are the acceleration due to gravity, the coefficient of thermal expansion and the viscosity, respectively. The velocity of propagation of the pinch on figures 2 and 3 is given using the above scaling. The Prandtl number dependence is evident in figure 3 in conjunction with the above scaling, which implies that acceleration is an important dynamical ingredient in the propagation of the pinch mechanism. Therefore, although it is customary to say that acceleration is completely negligible in fluids with a Prandtl number close to 10^4 , this evidence shows the contrary.

One can take the curl of the above Navier-Stokes equation to arrive at a vorticity equation. The vertical vorticity, in the $\hat{\mathbf{k}}$ direction, can be only of order Pr^{-1} because it can be produced only by nonlinear terms, the curl of the body force due to the temperature having no component in the $\hat{\mathbf{k}}$ direction. Quite possibly vertical vorticity is in fact generated by such dislocations. Relevant to this is the fact that Chen & Whitehead described some size-adjustment mechanisms due to walls at the edge of the container and it is known that such walls do produce a component of vertical vorticity. If vertical vorticity does play an important part in these problems, a degree of freedom which is not liberated by uniform Bénard convection planforms to the lowest order is liberated by flaws, and hence they serve a particularly interesting purpose.

One might inquire whether there is any gross characteristic of the system towards which the pinches drive the convection. Krishnamurti (1970) reports that rolls tend to cluster around the left-hand stability curve derived by Busse (1967) if the system is given enough time to come to a steady state. This is

compatible with our observations that pinches drive rolls towards large wavelengths.

We can estimate the heat transport, kinetic energy and temperature variation as a function of wavelength, using coefficients for the various harmonics of finite amplitude convection between rigid boundaries calculated by Busse (1967). The actual constants were kindly supplied by Busse. Figure 4 shows the estimated values of these properties, suitably normalized, as a function of wavelength at a Rayleigh number of 10 000. The values of the heat transport, kinetic energy and temperature fluctuation were estimated using the formulae

$$H \simeq \sum_{\nu=1}^8 \nu \pi b_{0\nu},$$

$$\text{KE} = \frac{1}{8} \int_{-\frac{1}{2}}^{\frac{1}{2}} \sum b_{\lambda\nu} b_{\lambda l} \left[\lambda^2 \alpha^2 \frac{\partial v_\nu}{\partial z} \frac{\partial v_l}{\partial z} + \lambda^4 \alpha^4 v_\nu v_l \right] dz,$$

$$\langle \theta^2 \rangle = \frac{1}{4} \sum b_{\lambda\nu}^2.$$

Symmetry dictates that even terms contribute to the first series. Busse showed that inclusion of the tenth term changes the heat transport by less than 1%. The second formula, for kinetic energy, contains an integral which was integrated numerically on a computer in two different ways after checking both programs against a test function with a known integral. The function v_ν is given after equation (4) in Busse's paper. All terms for which $\lambda + \nu \leq 8$ and $\lambda + l \leq 8$ were included in the summation. The third formula, for $\langle \theta^2 \rangle$, is obtained by straightforward integration of Busse's equation (4). Again, all terms with $\lambda + \nu \leq 8$ are included in the summation.

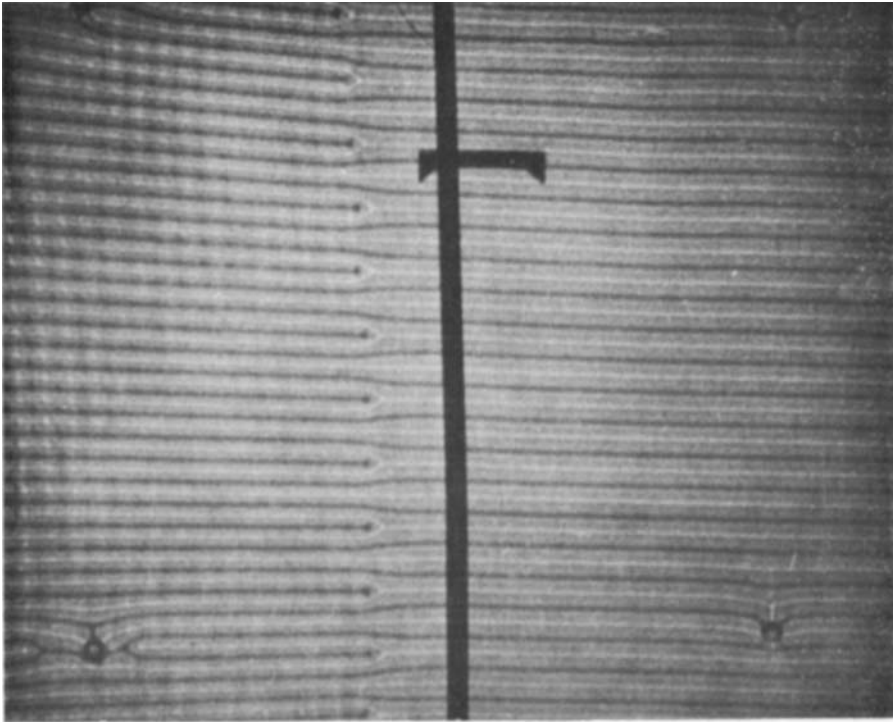
In order to enhance the visualization of the maxima, constants have been subtracted from the kinetic-energy and temperature-fluctuation terms.

We remind the reader that heat transport, total entropy production, buoyancy work and viscous dissipation are all equivalent for the steady-state convection. The arrow corresponds to the wavenumber $\alpha = 2.36$, below which the rolls become unstable as predicted by Busse (1967). It appears that pinches drive rolls towards this point. In view of the fact that others have observed wavelengths of random convection in this region, it appears that dislocations drive the convection parameters off both the heat-transport and the kinetic-energy maximum towards a region of parameter space where the fluid possesses a greater variation of temperature. It also appears that nonlinearities in the Navier-Stokes equation play at least some role in this.

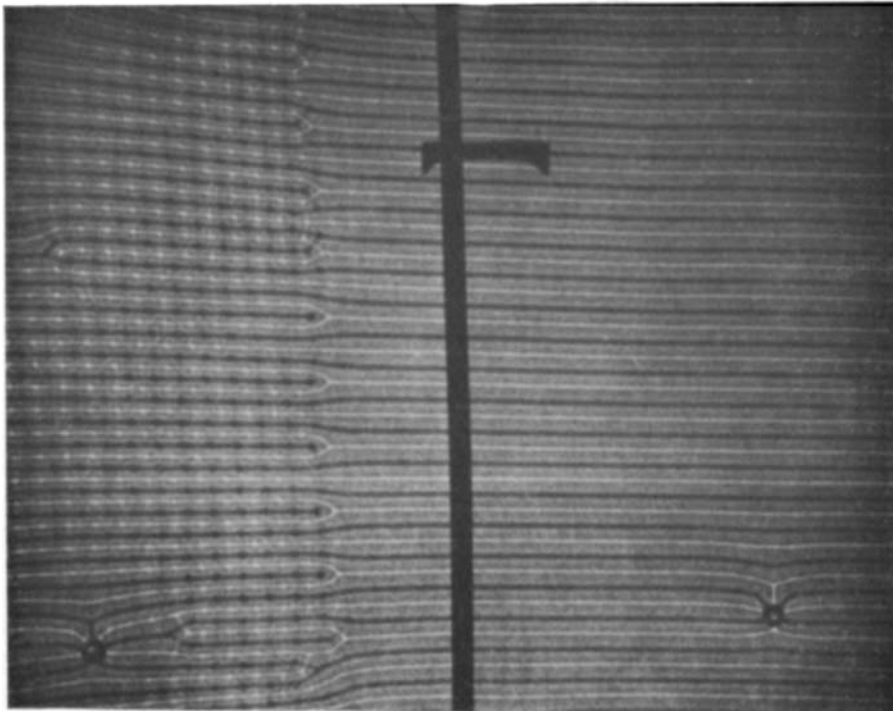
REFERENCES

- BUSSE, F. 1967 On the stability of two-dimensional convection in a layer heated from below. *J. Math. & Phys.* **46**, 140–150.
- BUSSE, F. & WHITEHEAD, J. A. 1971 Instabilities of convection rolls in a high Prandtl number fluid. *J. Fluid Mech.* **47**, 305–320.
- BUSSE, F. & WHITEHEAD, J. A. 1974 Oscillatory and collective instabilities in large Prandtl number convection. *J. Fluid Mech.* **66**, 67–79.
- CHEN, M. M. & WHITEHEAD, J. A. 1968 Evolution of two-dimensional periodic Rayleigh convection cells of arbitrary wave-numbers. *J. Fluid Mech.* **31**, 1–15.

- KOSCHMIEDER, E. L. 1966 On convection on a uniformly heated plane. *Beitr. Phys. Atmos.* **39**, 1–11.
- KOSCHMIEDER, E. L. 1969 On the wavelength of convective motions. *J. Fluid Mech.* **35**, 527–530.
- KOSCHMIEDER, E. L. 1974 Bénard convection. *Adv. Chem. Phys.* **26**, 177–212.
- KRISHNAMURTI, R. 1970 On the transition to turbulent convection. Part 1. The transition from two- to three-dimensional flow. *J. Fluid Mech.* **42**, 205–307.
- LIPPS, F. B. & SOMERVILLE, R. C. J. 1971 Dynamics of variable wavelength in finite-amplitude Bénard convection. *Phys. Fluids*, **14**, 759–765.
- ROSSBY, H. T. 1969 Bénard convection with and without rotation. *J. Fluid Mech.* **36**, 309–335.
- WILLIS, G. E., DEARDOFF, J. W. & SOMERVILLE, R. C. J. 1972 Roll-diameter dependence in Rayleigh convection and its effect upon the heat flux. *J. Fluid Mech.* **54**, 351–367.



(a)



(b)

FIGURE 1. Photographs of rolls with a wavenumber of 2.46 which contract to rolls with wavenumbers 3.69 by means of the pinch mechanism. (a) The convection just as it is approaching the final steady temperature difference to give a Rayleigh number of 20 000. (b) The convection 41 min later, with bimodal flow in the smaller wavelength rolls. The thermal time constant d^2/κ of this fluid is 21 min.